Measurement of Protein Diffusion in Dextran Solutions by Holographic Interferometry

T. Fettah Kosar and Ronald J. Phillips
Dept. of Chemical Engineering and Materials Science, University of California, Davis, CA 95616

Theories and experimental measurements related to the diffusion of globular macromolecules and small spheres in polymer solutions are discussed. It is shown that the Kirkwood-Riseman point scatterer and Brinkman models, two theoretical approaches that lead to hydrodynamic screening, are equivalent. Holographic interferometry is presented as a new method for measuring gradient diffusion of proteins in transparent polymer solutions and gels. This method is used to examine the effect of ionic strength, polymer concentration and polymer molecular weight on the diffusion of bovine serum albumin (BSA) in dextran solutions. The data are interpreted in light of the hydrodynamic screening and Stokes-Einstein models of diffusion. In particular, it is shown that while the Stokes-Einstein equation may be appropriate for the diffusion of relatively large latex spheres in polymer solutions, it is inappropriate for predicting diffusion coefficients of BSA and comparable proteins in such solutions.

Introduction

The diffusion of proteins and colloidal particles in polymer solutions is nearly always slower than in the pure solvent. Studies of diffusion in these systems are of use both for improving models of polymer dynamics in solution and for gaining a better understanding of diffusion in biological fluids, many of which contain dissolved polymers. Although the physical mechanisms used to explain this reduction in transport rate vary, most of the available data can be described empirically by the equation:

$$\frac{D}{D_0} = \exp(-\alpha\phi^{\nu}), \tag{1}$$

where the Stokes-Einstein diffusivity in pure solvent D_0 is given by:

$$D_0 = \frac{k_b T}{6\pi\eta_0 a}. \tag{2}$$

In Eqs. 1 and 2, ϕ is the polymer volume fraction, k_b is Boltzmann's constant, T is absolute temperature, and a is the solute radius. The parameters α and ν are generally calculated so as to obtain the best fit with experimental data. Equation 1 has been termed a "stretched exponential," and has been used by numerous researchers to correlate data (Laurent et al., 1961; Laurent and Persson, 1963; Ogston et al., 1973; Turner and Hallett, 1976; Phillies et al., 1989; Phillies and Clomenil, 1993; Tracy and Pecora, 1993).

Although it is widely agreed that Eq. 1 is very successful in fitting diffusion data in polymer solutions, there is less agreement on theories for the prediction and interpretation of the parameters α and ν. It is therefore useful to reexamine the theoretical underpinnings of that equation. Some of the more rigorous derivations of rates of diffusion in polymer solutions rely on a Kirkwood-Riseman type of model, in which a spherical solute is surrounded by fluid containing immobile point singularities (Freed and Muthukumar, 1978; Cukier, 1984; Altenberger et al., 1986). The point singularities serve as centers of hydrodynamic resistance, and model polymer fibers that are held fixed in place by entanglements with other macromolecules. Summation of the contributions of the point singularities leads to an expression for the enhanced drag on the solute, yielding a hindered diffusion coefficient of the form:

$$\frac{D}{D_0} = 1 - \alpha\phi^{1/2}. \tag{3}$$

The theoretical value of the parameter α is $\sqrt{2}/3$ for point

Correspondence concerning this article should be addressed to R. J. Phillips.

singularities representing a dilute medium of spheres with radii equal to the solute radius. For the more general case where the radii differ, α depends on the ratio of the solute radius and the "fiber" radii. Cukier (1984) points out that Eq. 3 is equivalent to Eq. 1 with $\nu = 0.5$ in the limit $\phi \ll 1$, and provides a phenomenological derivation of Eq. 1 based on the assumption that incremental increases in the polymer volume fraction ϕ have a similar effect on diffusion for all values of ϕ.

Phillips et al. (1989; 1990) suggest an alternate form of Eq. 3 that is obtained by solving Brinkman's equation, which yields

$$\frac{D}{D_0} = \frac{1}{1 + \frac{a}{\sqrt{k}} + \frac{1}{3}\left(\frac{a}{\sqrt{k}}\right)^2}, \tag{4}$$

where k is the hydraulic permeability of a fibrous medium with volume fraction ϕ. For a dilute medium of randomly dispersed spheres with radius a, the hydraulic permeability k is given by:

$$k = \frac{9}{2\phi}\, a^2, \tag{5}$$

and Eqs. 3 and 4 are therefore identical to $O(\phi^{1/2})$, both in terms of the functional dependence on volume fraction and the numerical value of the parameter α. We note, however, that the $O(\phi)$ term, which corresponds to the squared term in the denominator of Eq. 4, depends on the local microstructure as discussed by Kim and Russel (1985). Equation 4 does not account for local microstructure, and is therefore expected to be most accurate when $a/\sqrt{k} \ll 1$. The formal equivalence of the Kirkwood-Riseman and Brinkman models is shown in the next section. Phillips and co-workers compare the predictions of Eq. 4 with rigorous calculations of hindered diffusion *coefficients* in a spatially periodic array of fibers, and find generally good agreement. They also use the experimentally measured values of k provided by Ethier (1986) to predict values of D/D_0 for several proteins in hyaluronic acid solutions. Interestingly, the predictions agree very closely with the results of Laurent et al. (1963), Laurent and Persson (1964), and Ogston et al. (1973), even without the use of adjustable parameters.

In spite of the fact that the Brinkman or hydrodynamic screening theories are in good agreement with some diffusion data, they are in apparent disagreement with other experimental results. In particular, a number of light scattering studies (Turner and Hallett, 1976; Phillies et al., 1989; Pu and Brown, 1989; Phillies and Clomenil, 1993; Onyenemezu et al., 1993) suggest that the ratio D/D_0 for probe diffusion in polymer solutions is independent of solute size, and follows the Stokes-Einstein prediction:

$$\frac{D}{D_0} = \frac{\eta_0}{\eta}. \tag{6}$$

This result suggests that the primary effect of adding polymer to a solvent is to increase the viscosity, resulting in a reduction in the diffusivity as calculated by Eq. 2. We note here that Eq. 6 is predicted in the limit of large solutes by the theory of Langevin and Rondelez (1978) (see also Tracy et al., 1993). Also, there is evidence that the Stokes-Einstein prediction does not apply equally well to all polymer/probe systems (Brown and Rymden, 1986, 1987; Mustafa and Russo, 1989; Phillies, 1989; Phillies and Clomenil, 1993). However, the clear difference between Eq. 6 on the one hand and Eqs. 3 and 4, which do predict a dependence on solute size, on the other, provides strong motivation for further experimental and theoretical study of this important problem, particularly when one considers that both equations can be supported by experimental data.

We have measured rates of diffusion of the protein bovine serum albumin (BSA) in solutions of dextran by holographic interferometry. This method has been used previously to measure diffusion of sugars in pure liquids (Bochner and Pipman, 1976; Gabelmann-Gray and Fenichel, 1979; Szydlowska and Janowska, 1982; Seufert and O'Brien, 1984) and in calcium alginate gels (Ruiz-Bevia et al., 1989), but has not yet been applied to the study of protein diffusion or to the study of diffusion in polymer solutions. We present results for protein diffusion in solutions of dextran with molecular weights from 9,000 to 2,000,000, and in concentrations ranging from 0 to 7.5% by weight. Also included is data on BSA diffusion as a function of ionic strength, viscosities of the polymer solutions to be used in conjunction with Eq. 6, and results for the diffusion of the dextran molecules themselves in the absence of protein.

In this article, the equivalence of the Kirkwood-Riseman and Brinkman models is demonstrated, thereby showing the close relationship between derivations based on point scatterers (Freed and Muthukumar, 1978; Altenberger et al., 1986) and those based on Brinkman's equation (Cukier, 1984; Phillips et al., 1989). The theory and experimental apparatus needed to measure diffusion by holographic interferometry are then presented, our experimental results are given, and we conclude with a discussion of our results in light of the theories mentioned above.

Equivalence of the Brinkman and Kirkwood-Riseman Models

We consider a spherical solute with radius a moving with velocity U through a polymer solution which we model as a medium of point scatterers. The fluid outside the solute is therefore governed by the equation

$$\nabla^2 \hat{v} - \nabla \hat{p} = -\sum_i \delta(\hat{r} - \hat{r}_i)\hat{F}_i, \tag{7}$$

where $\hat{v}$ is the fluid velocity normalized by the sphere velocity U, $\delta(\hat{r} - \hat{r}_i)$ is the Dirac delta function and $\hat{F}_i$ is the dimensionless force required to hold the ith sphere (singularity) motionless. The force $\hat{F}_i$ is made dimensionless by $\eta_0 a U$, and the singularity positions $\hat{r}_i = r_i/a$ are random and extend to infinity. In order to determine the diffusion coefficient of the spherical solute, we first solve Eq. 7 in order to calculate the increase in the hydrodynamic drag owing to the scatterers. We then modify accordingly the drag coefficient that constitutes the denominator of Eq. 2. We note that in taking this approach we are neglecting electrostatic interactions, which may be important in some systems. However, hydrodynamic interactions decay more slowly than electrostatic interactions in an aqueous

solution of moderate ionic strength, and we therefore expect hydrodynamics to be the dominant influence in many systems of interest.

The solution to Eq. 7 can be written as a sum of Stokes flow around the moving sphere plus the contributions of the singularities:

$$\hat{v}(\hat{r}) = \hat{v}_s(\hat{r}) + \hat{v}'(\hat{r}|C_N), \tag{8}$$

where $\hat{v}_s$ is the velocity field for Stokes flow around a sphere and $\hat{v}'(\hat{r}|C_N)$ is the perturbation field caused by the N singularities in the configuration C_N. The effect of the perturbation fields can be calculated by direct summation (Freed and Muthukumar, 1978; Altenberger et al., 1986), using the assumption that the singularities are evenly distributed in space. Here we show that the result obtained by the direct summation approach, when averaged over possible configurations of the singularities, yields exactly the result found by solving Brinkman's equation.

Using the nomenclature of Batchelor (1972), we ensemble average Eq. 8 by multiplying by the probability $P(C_N)$ of the configuration C_N and integrating over all configurations, yielding

$$\langle \hat{v} \rangle (\hat{r}) = \hat{v}_s(\hat{r}) + \frac{1}{N!} \int \hat{P}(C_N) \hat{v}'(\hat{r}|C_N) dC_N. \tag{9}$$

Here the probability has been made dimensionless according to $\hat{P}(C_N) = a^{3N} P(C_N)$. The total velocity perturbation $\hat{v}'(\hat{r}|C_N)$ in Eq. 9 can be expressed as a sum of the perturbations $\hat{v}'_i(\hat{r}|\hat{r}_i)$ caused by each of the N singularities. Also, for dilute media the probability is given approximately by:

$$\hat{P}(C_N) = \hat{P}(r_i)\hat{P}(C_{N-1}|r_i) \approx \hat{P}(r_i)\hat{P}(C_{N-1}). \tag{10}$$

Substituting these results into Eq. 9 and integrating over configurations of N-1 singularities gives

$$\langle \hat{v} \rangle (\hat{r}) = \hat{v}_s(\hat{r}) + \frac{1}{N} \sum_{i=1}^{N} \int d\hat{r}_i \hat{P}(\hat{r}_i) \hat{v}'(\hat{r}|\hat{r}_i). \tag{11}$$

Then, since all the singularities have identical scattering properties,

$$\langle \hat{v} \rangle (\hat{r}) = \hat{v}_s(\hat{r}) + \int d\hat{r}_i \hat{P}(\hat{r}_i) \hat{v}'(\hat{r}|\hat{r}_i), \tag{12}$$

where the subscript i denotes the position of any singularity. Equation 12 states that the average velocity at $\hat{r}$ is the velocity field for Stokes flow around a sphere plus the velocity perturbation of a singularity at $\hat{r}_i$, multiplied by the probability there is a singularity at $\hat{r}_i$, integrated over space.

The velocity perturbation $\hat{v}'(\hat{r}|\hat{r}_i)$ can be expressed in terms of the average velocity by first noting that

$$\hat{v}'(\hat{r}|\hat{r}_i) = \hat{G}(\hat{r},\hat{r}_i) \cdot \hat{F}_i. \tag{13}$$

Here $\hat{G}$ is the Green's function which gives the velocity disturbance at $\hat{r}$ caused by a singularity at $\hat{r}_i$. This velocity disturbance must match the boundary conditions on the surface of the sphere; such a Green's function for a singularity near a sphere can be derived (Kim and Karrilla, 1991), but the exact form is not necessary for this derivation. Assuming the force is related to the average velocity by a drag coefficient $\hat{K}$ and substituting into Eq. 12, one finds

$$\langle \hat{v} \rangle (\hat{r}) = \hat{v}_s(\hat{r}) + \int d\hat{r}_i \hat{G}(\hat{r},\hat{r}_i) \cdot (\hat{n}\hat{K} \langle \hat{v} \rangle (\hat{r}_i)), \tag{14}$$

where it has been assumed that medium around the solute is homogeneous so the probability $\hat{P}(\hat{r}_i)$ is equal to the number density of singularities $\hat{n}$.

As pointed out by Wiegel (1980) and Rubinstein (1986), Eq. 14 is just the integral solution to the equation

$$\nabla^2 \hat{v} - \nabla \hat{p} = -\hat{f}, \tag{15}$$

where the body force $\hat{f}$ is equal to $\hat{n}\hat{K}\langle \hat{v} \rangle$. Equation 15 is of course just Brinkman's equation. For a dilute medium of spheres, the drag coefficient K is $6\pi\eta a$ and the hydraulic permeability k is given by:

$$k = \frac{\eta}{nK} = \frac{9a^2}{2\phi}, \tag{16}$$

which is the same as the result given in Eq. 5. The length scale $k^{1/2}$ is known as the Brinkman screening length, and is a characteristic length for the propagation of velocity disturbances in media governed by Eq. 15. It has also recently been shown that this same length scale is evident in suspensions of rigid fibers (Shaqfeh and Fredrickson, 1990), a topic discussed in more detail in the discussion section. We conclude that the Kirkwood-Riseman approach of summing the contributions of the individual singularities and averaging over possible configurations is no different from solving Brinkman's equation, at least in the limit of low polymer volume fraction.

The fact that the problem of a spherical solute in an infinite polymer solution is unbounded makes it difficult to perform numerical calculations by using Eq. 14, particularly in light of the slow decay of scattered velocity perturbations in the absence of boundaries. The principal causes of these difficulties are discussed by Kim and Russel (1985). However, it is possible to demonstrate the equivalence of Brinkman's equation 15 and Eq. 14 by considering the bounded problem of flow through a partially or completely polymer-filled cylindrical tube, as shown in Figure 1. For a completely filled pore, the singularity positions are random and extend to infinity in the axial direction. For a partially filled pore, the density of singularities is still constant in the angular and axial directions, but they are located only in the finite region adjacent to the pore wall where $R < r_i < R_0$.

We rewrite Eq. 14 as the sum of a parabolic imposed flow $\hat{v}_p$ and the contributions of the singularities, which are again written in integral form, to find

$$\langle \hat{v} \rangle_z (\hat{r}) = \hat{v}_p(\hat{r}) + \int d\hat{r}_i \hat{P}(\hat{r}_i) \hat{G}_{zz}(\hat{r},\hat{r}_i) (\hat{K} \langle \hat{v} \rangle_z (\hat{r}_i)), \tag{17}$$

where it has been assumed that the radial and angular components of the average velocity are zero for probability densities that vary only in the radial direction. Here the Green's

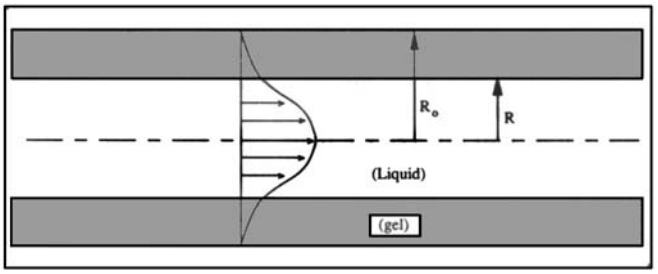

Figure 1. Cylindrical pore geometry.

function $\hat{G}$ is that for flow in a cylindrical tube, and therefore matches the no slip condition on the tube wall. Expressions for all the components of $\hat{G}$ have been evaluated by Liron and Shahar (1978).

Equation 17 is an integral equation for the average velocity. It is solved by evaluating the axial and angular portions of the integral on the right side analytically, using the solution of Liron and Shahar for the Green's function $\hat{G}$. The radial portion of the integral is then discretized according to Simpson's rule, resulting in a set of linear equations for the unknown velocity profile. Since the gel is assumed to be homogeneous, the probability $\hat{P}$ is equal to a constant $\hat{n}$ for the completely filled pore, and is given by

$$\hat{P}=0 \quad 0\le\hat{r}\le\hat{R} \tag{18a}$$

$$\hat{P}=\hat{n} \quad \hat{R}\le\hat{r}\le 1 \tag{18b}$$

for the partially filled pore. Here radial positions have been made dimensionless by R_0, the pore radius, and $\hat{n}=nR_0^3$. The value of $\hat{K}$ is given by the drag coefficient for a sphere in a dilute array of identical spheres (Freed and Muthukumar, 1978; Kim and Russel, 1985)

$$\hat{K}=6\pi\left(1+\frac{3}{\sqrt{2}}\phi^{1/2}\right). \tag{19}$$

Equation 19 is derived without making use of Brinkman's equation, and therefore its use does not compromise the independence of the singularity and Brinkman models under consideration here.

Velocity profiles that are calculated from Eq. 14 are presented in Figure 2 for pores completely filled with polymer. These profiles are compared with the Brinkman result, which is provided in analytical form by Ethier and Kamm (1989). Clearly the numerical computations confirm the equivalence of the Kirkwood-Riseman and Brinkman models, the two sets of results being identical for all three number densities shown, $\hat{n}=100$, 400 and 1,200. The transition from the parabolic velocity profile expected when no gel is present to the plug flow that is predicted by Darcy's law for flow through a porous medium is also readily apparent, particularly for the profile where $\hat{n}=1{,}200$. We note here that, for the purposes of computing the drag coefficient from Eq. 19, a sphere size of $a/R_0=0.01$ is used; however, the agreement between the Kirkwood-Riseman and Brinkman models shown in Figure 2 is not limited to particular values of that ratio, and was specifically verified for values as high as 0.1.

Predictions of the Brinkman and Kirkwood-Riseman models

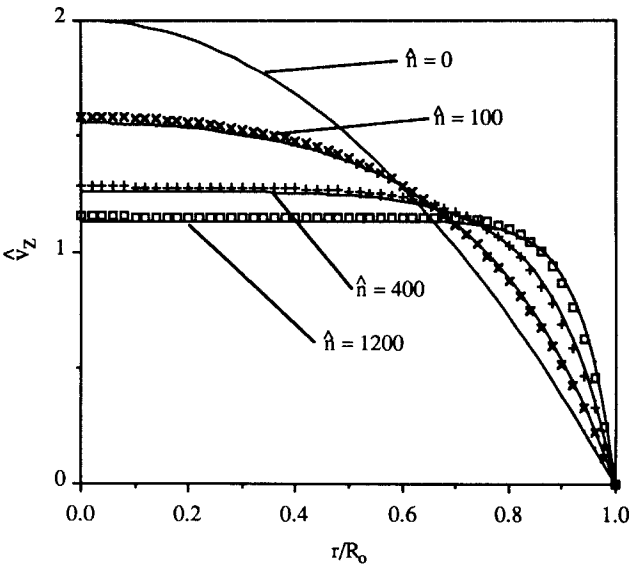

Figure 2. Velocity profiles in completely filled pore ($\hat{R}=0$) for a range of number densities $\hat{n}$.

Solid curves are results from Brinkman's Eq. 15. The parabolic profile corresponding to $\hat{n}=0$ is shown for comparison.

for flow through a partially-filled pore are shown in Figure 3. Here the pore is half-filled with polymer, $\hat{R}=0.5$, and the Brinkman result is again calculated using equations provided by Ethier and Kamm (1989). As in Figure 2, results are shown for number densities $\hat{n}=100$, 500 and 1,200 for a sphere size of $a/R_0=0.01$. In each case, the effect of the gel or polymer layer is to slow down the fluid near the wall, resulting in an inflection point before the velocity profile assumes a parabola-like shape in the core of the tube. Also as in Figure 2, the two models are nearly indistinguishable, a fact that is particularly interesting when one notes that there are both liquid/gel and gel/wall boundaries, with a rapid change in velocity clearly visible at the former. The results of Figures 2 and 3 are a clear

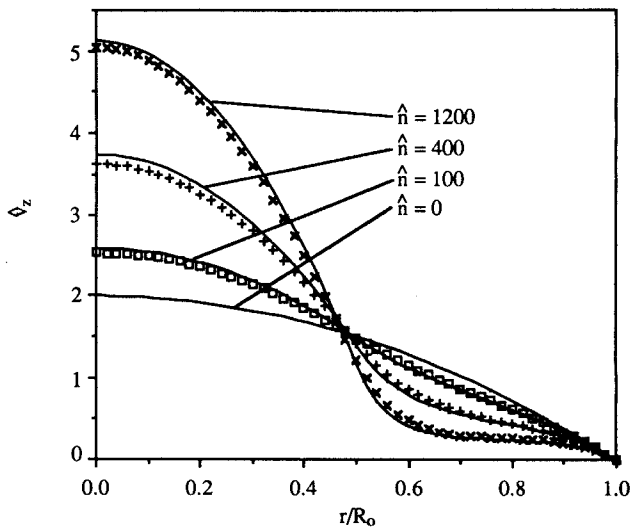

Figure 3. Velocity profiles in half-filled pore ($\hat{R}=0.5$) for a range of number densities $\hat{n}$.

Solid curves are results from Brinkman's equation; parabolic profile corresponding to $\hat{n}=0$ is again shown for comparison.

illustration of the fact that computing flows through a medium of point scatterers by summing the contributions of each singularity is essentially the same as solving Brinkman's equation. The use of Eq. 4 with the appropriate hydraulic permeability therefore provides a convenient way of obtaining results equivalent to Eq. 3, but for a fibrous or other medium with a microstructure that differs from a dilute, homogeneous array of point scatterers.

Measurement of Diffusion by Holographic Inteferometry

Evaluation of the usefulness of the Brinkman and other models of hindered diffusion is best performed by comparison with experimental data. Here we introduce holographic interferometry (HI) as a new method for measuring protein diffusion in polymer solutions, polymer gels, and other transparent media. The use of classic laser interferometry to measure rates of diffusion is well-established, and indeed some of the most accurate diffusion data available have been obtained by that method (Tyrell and Harris, 1984). To measure diffusion by classic interferometry, a beam of laser light is first passed through a beam splitter, which forms the test and reference beams. The test beam passes through a diffusion cell which contains a solute diffusing down a concentration gradient. The presence of the concentration gradient (and hence gradient in refractive index) in the diffusion cell changes the optical path length of the test beam relative to that of the reference beam. Thus, when the two beams are recombined they form a series of constructive and destructive interference fringes. The fringe shape and spacing are then used to determine the diffusion coefficient.

In holographic interferometry (HI) one uses the same principles of optical interference that are applied in classic interferometry. However, instead of having a separate reference beam, in HI one records the holographic image of the diffusion cell at a time t_1 and reconstructs that image at later times t_2, t_3 . . . , at which point the *reconstructed image* is used as the reference needed to form interference fringes. Thus, unlike traditional interferometers, holographic interferometers are *single-path* devices in that the test and reference beams both travel across the same space, but at different times. The interferograms constructed from these experiments therefore provide a measure of the temporal changes that occur as diffusion is taking place, and a relatively simple analysis allows one to use them to calculate diffusion coefficients.

The primary advantages of holographic as opposed to traditional interferometry arise from the fact that in HI the test and reference beams are guaranteed to be identical except for temporal changes that occur inside the diffusion cell. In other words, since the two beams are traveling across exactly the same paths, the only possible changes that can occur are caused by changes in the concentration profile resulting from diffusion. This property is in contrast to traditional interferometers in which, for example, slight defects or spatial variations in the glass wall of the diffusion cell can cause complicated interference patterns. This single-path characteristic makes alignment of the optics considerably easier in HI. It also eliminates the need for high quality, defect-free glass in the diffusion cell; simple glass spectrophotometric cuvettes perform very nicely in holographic interferometry. Finally, this same property makes HI suitable for measuring diffusion in complex media such as polymeric gels. In classic interferometry, the nearly unavoidable presence of minor inhomogeneities can make it very difficult to distinguish between interference fringes caused by minor inhomogeneities in the gel matrix and those caused by the diffusing solute. In HI, the use of the holographic image of the diffusion cell as a reference effectively eliminates any difficulties caused by the inhomogeneities in the gel matrix.

Measuring rates of diffusion in polymer solutions and gels by holographic interferometry requires further study before detailed comparisons with noninterferometric methods can be made. However, certain features of HI make it an attractive alternative that complements other methods such as fluorescence recovery after photobleaching (FRAP) (Jain et al., 1990), holographic relaxation spectroscopy (HRS) (Stewart et al., 1988) and dynamic light scattering (Phillies et al., 1989). First, unlike FRAP and HRS holographic interferometry provides a direct, noninvasive way of monitoring diffusion down a macroscopic, imposed concentration gradient, or gradient diffusion, as opposed to self or tracer diffusion processes which do not involve concentration gradients. Since it is the gradient diffusion coefficient that governs the macroscopic flux, being able to measure it directly could be of use in certain circumstances. Also, as pointed out by Tracy and Pecora (1992), in polymer gels light scattering time-average intensity autocorrelation functions taken at a single localized region are not necessarily representative of the entire gel. In contrast, monitoring the concentration change over a macroscopic region, as done in HI, insures that one is measuring an ensemble averaged diffusion coefficient. Finally, the analysis of interference fringes is very simple as shown below, and requires only the assumption of Fick's law of diffusion, unlike the relatively involved analyses required in dynamic light scattering (Berne and Pecora, 1990). Thus, straightforward interpretation of data is possible even in highly complex media.

In addition to the diffusion of proteins in polymer solutions considered here, we anticipate being able to use HI to measure the diffusion of micelles in polymer solutions and polymer gels, or the diffusion of any solute in a mixed medium of polymers (either in solution or cross-linked) and micelles. Alternatively, with some modifications the distribution of solutes moving through a gel by convection or by electrophoresis can be monitored. Thus, holographic interferometry provides interesting possibilities for measuring diffusion, and can also be applied to the study of other important transport processes.

Experimental apparatus and procedure

A diagram of our holographic interferometry apparatus is shown in Figure 4. The beam from a 10 mW HeNe laser (Newport, Irvine, CA) is focused through a pinhole spatial filter by a 10X microscope objective and split by a variable beam splitter (Newport, Irvine, CA). The primary or "object" beam is then passed through a collimating lens with focal length 15 in. (381 mm) (Space Optics Research Labs, Chelmsford, MA) and reflected off a 2 in. dia. (51 mm) mirror (New Focus, Mountain View, CA) before it traverses the diffusion cell and impinges on the holographic plate. The duration of the exposure of the holographic plate is controlled by an electronic shutter (Newport, Irvine, CA). The second beam emitted from the beam splitter is collimated and reflected in the same way as the object beam, and is necessary for the exposure of the holographic plate; it is *not* a reference beam in the sense of

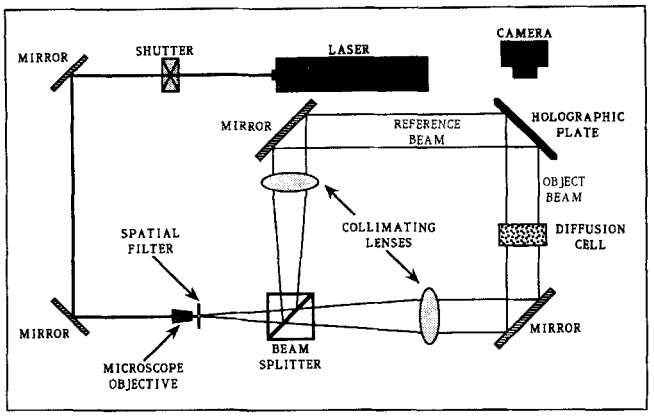

Figure 4. Apparatus for holographic interferometry.

traditional interferometry. The holographic images are recorded on Agfa Holotest holographic plates, and the interference fringes are photographed with a Nikon N6000 camera with a 105 mm lens. The entire experimental apparatus is mounted on an 8 ft × 4 ft × 8 in. (2.4 m × 1.2 m × 203 mm) optical table (Newport, Irvine, CA) that is isolated from vibrations by pneumatic legs. The apparatus is located in a room with the temperature controlled at 23±2°C.

The diffusion cell is a 4 cm × 1 cm × 5 mm spectrophotometric cuvette with a 5 mm light path. The solute-depleted solution is added first, and the solute-rich solution follows so that the more dense liquid is on the bottom. The latter, solute-rich solution is introduced by using a syringe pump to force the liquid through a capillary tube glued to one corner, with the outlet of the tube being at the bottom of the cuvette. We find that maintaining a discrete interface between the two liquids is not difficult provided the filling process is performed slowly. Our filling times range from approximately 30 to 90 min, and the interface remains flat during the entire process. The initial time t_0 is taken to be the beginning of the time of the filling, when the interface is first formed. It is important to note that disruptions in the interface are immediately obvious to the experimentalist, and the absence of a clear interface makes it impossible to get interference fringes of the type shown in the experimental results section. Thus, this method makes it quite easy to detect a failed experiment. Our BSA and dextran were purchased from Sigma (Saint Louis, MO), and were used as supplied. The molecular weights reported are the nominal values.

The exposure of the holographic plate takes place typically 1-4 h after the start of the filling process. The duration of the exposure of the holographic plate is approximately 0.1 s for the systems studied here. The plate is then removed from the plate holder (Newport, Irvine, CA), developed, and replaced back into the plate-holder, which is designed so as to allow the plate to be returned precisely to its original position. For reasons to be described below the object beam is now tilted slightly in the horizontal direction, and the interference fringes are photographed at regular intervals. A more detailed description of the experimental apparatus and procedure can be found in Kosar (1993).

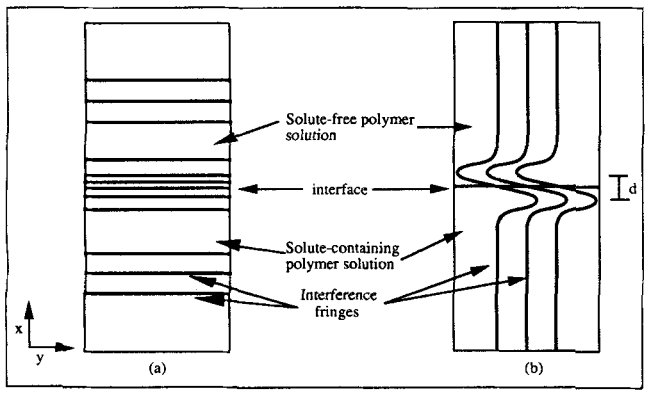

Figure 5. Interference patterns obtained (a) before and (b) after tilting the object beam.

Analysis of interference fringes

A diagram of interference patterns obtained by the above procedure is shown in Figure 5. As mentioned, part of that procedure involves tilting the object beam after the exposure of the holographic plate at time t_1 and before taking photographs of the interference patterns at later times t_2, t_3, . . . Before tilting the object beam, the optical path length varies only in the x-direction, which is the direction of the diffusive solute flux. Horizontal fringes are therefore visible, as shown in Figure 5a. The fringes are located at points where the concentration change ΔC is sufficient to change the optical path length by odd multiples of one-half of the wavelength, thereby causing destructive interference. Here ΔC is the concentration change from the time of exposure of the holographic plate to the time of observation of the fringes. Tilting the object beam by a small angle α introduces a y-dependence in the optical path length, and causes the fringes to change shape as shown in Figure 5b.

The exact shape of this interference pattern can be predicted theoretically by noting that dark fringes form where the irradiance, or intensity of light, is zero. The irradiance I is found by adding the holographically stored light wave from time t_1 to actual light passing through the sample at the later time t_2, and has the form

$$I = A^2 \cos\left[k_\lambda(\Delta n_r - \alpha y)\right], \tag{20}$$

where A is the amplitude of the light wave, k_λ is the wave number and Δn_r is the change in refractive index between times t_1 and t_2. The irradiance is zero when the argument of the cosine in Eq. 20 is a constant equal to an odd multiple of $\pi/2$. Assuming concentration and refractive index are linearly related, as is the case for concentration changes that are not too large, it is then a simple matter to show that the fringe position y and the concentration change ΔC are linearly related, or that

$$y = m\Delta C + b, \tag{21}$$

where m and b are constants that need not be specified.

As illustrated in Figure 5b, the fringes trace out maximum and minimum values of y at specific values of x. The vertical distance between these extrema depends on the concentration change from time t_1 to time t_2. An exact expression relating the distance d between the extrema, the times t_1 and t_2 and the

diffusion coefficient D can be found by evaluating ΔC, differentiating y in Eq. 21 with respect to x and setting the result equal to zero. The problem that must be solved in order to calculate ΔC as a function of position and time is

$$\frac{\partial C}{\partial t} = D\frac{\partial^2 C}{\partial x^2} \tag{22}$$

with the initial conditions

$$C_1(x,0) = 0 \text{ for } x > 0 \tag{23}$$

$$C_2(x,0) = C_0 \text{ for } x < 0 \tag{24}$$

together with the boundary and matching conditions

$$C_1(\infty,t) = 0 \tag{25}$$

$$C_2(-\infty,t) = C_0 \tag{26}$$

and

$$C_1(0,t) = C_2(0,t) \tag{27}$$

$$\frac{\partial C_1}{\partial x}(0,t) = \frac{\partial C_2}{\partial x}(0,t). \tag{28}$$

Here C_1 is the concentration of solute in the upper, initially solute-free solution and C_2 is the concentration in the lower solution. Solving Eq. 22 subject to the conditions of Eqs. 23–28 yields the following expression for the concentration change from time t_1 to time t_2 at some position x:

$$\Delta C = \frac{1}{2}\left(\text{erf}\left(\frac{x}{\sqrt{4Dt_1}}\right) - \text{erf}\left(\frac{x}{\sqrt{4Dt_2}}\right)\right)C_0, \tag{29}$$

where erf(ξ) is the error function. Substitution of Eq. 29 into Eq. 21 and differentiating to find the position of the maxima yields the desired expression that is used to find D (Bochner and Pipman, 1976; Szydlowska and Janowska, 1982):

$$D = \frac{d^2}{8}\frac{\left(\frac{1}{t_1} - \frac{1}{t_2}\right)}{\ln\left(\frac{t_2}{t_1}\right)}. \tag{30}$$

Note that this result is independent of factors like the thickness of the cell, the wavelength of the laser light, or the coefficient relating concentration and refractive index.

Practical application of holographic interferometry requires that diffusion coefficients be large enough so that the duration of an experiment is feasible. A typical experiment in which we measure a diffusion coefficient of 2.5×10^{-7} cm^2/s takes approximately 8 h, with t_1 being 3 h, t_2 being 8 h and a value of d equal to approximately 1.8 mm, as can be calculated from Eq. 30. Our values of d are measured on enlarged photographs, and require a distance between extrema of approximately this magnitude. Since diffusion time scales with the inverse of D, accurate measurements of smaller diffusion coefficients require longer experiments. However, the time required for an experiment can be controlled somewhat by changing t_1 and t_2. For example, to measure a diffusion coefficient of 1×10^{-7} cm^2/s, one could use times of 9 and 14 hours or 10 and 20 h for t_1 and t_2 and still have acceptable peak-to-peak separations. In general the shorter experiment will yield somewhat flatter extrema, making it more difficult to get accurate results. We have not done a careful study to determine the minimum amount of time to measure a given rate of diffusion, but such times can at least be estimated from Eq. 30.

In addition to these time requirements, the refractive index n_r must be sensitive enough to concentration variations to alter the vertical interference fringes by an amount sufficient to enable one to measure d and apply Eq. 30. In general, small changes in refractive index can be compensated for by increasing the optical path length. Let L be the optical path length of a given cell. Then the difference between the distances traveled by optical waves at times t_0 and t_1 (that is, the times when the holographic plate is exposed and the photograph is taken, respectively), when the refractive index has changed from $n_{r,0}$ to $n_{r,1}$, is $L(1\text{-}n_{r,1}/n_{r,0})$. Setting this change in optical path length equal to one-half the wavelength of the HeNe laser, 316 nm, yields a condition for the formation of a *horizontal* fringe such as those shown in Figure 5a. This condition is easily met even in dilute conditions, such as a 1% change in sucrose concentration in a cuvette with a 5 mm path length. However, the deformation of the *vertical* fringes needed to measure diffusion coefficients by application of Eq. 30 occurs even when the condition needed for formation of horizontal fringes is not met. In other words, the extrema shown in Figure 5b are visible even when the concentration-induced change in optical path length is less than half of one wavelength. We therefore feel that it is unlikely that future applications of holographic interferometry will be limited by a requirement for higher changes in refractive index. Although we have not tested the limits of our apparatus, we have had no difficulty measuring rates of diffusion in 0.5% BSA solutions using a spectrophotometric cuvette with a 5 mm path length.

Experimental Results

The procedure described above for measuring rates of diffusion yields accurate results for many different solutes and solutions. We tested our apparatus and experimental technique by first measuring rates of sucrose diffusion in water. For this experiment, the lower solution ($x<0$) is 10% sucrose by weight, while the upper solution ($x>0$) is pure deionized water. Our value for D at 23°C is 5.52×10^{-6} cm^2/s, which compares favorably with the results 5.56×10^{-6} cm^2/s and 6.0×10^{-6} cm^2/s that were obtained at 25°C by Bochner and Pipman (1976) and Gabelmann-Gray and Fenichel (1979), who also used holographic interferometry. Our diffusion coefficient is also quite close to the value of 5.21×10^{-6} cm^2/s given in the CRC *Handbook of Chemistry and Physics* (Weast and Astle, 1980).

Diffusion coefficients for the protein BSA in KCl solutions with varying ionic strengths are shown in Figure 6. The concentration of BSA used in the solute-containing solution is 1% by weight. The results show a dramatic increase in D/D_0 as the ionic strength of the solution is decreased, suggesting that

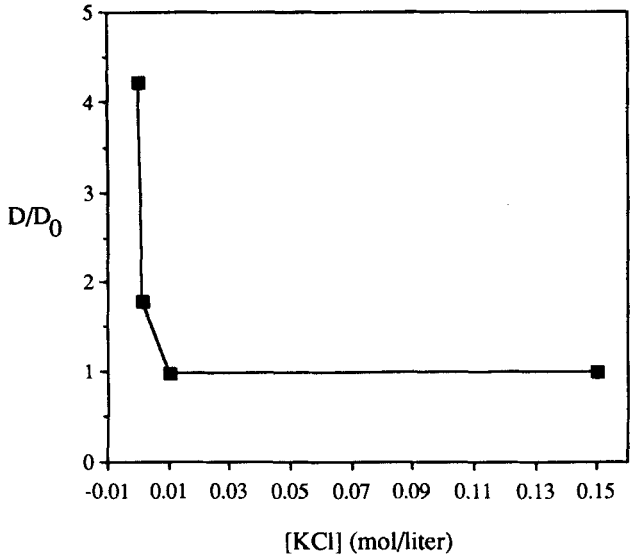

Figure 6. Effect of salt concentration on gradient diffusion of BSA.

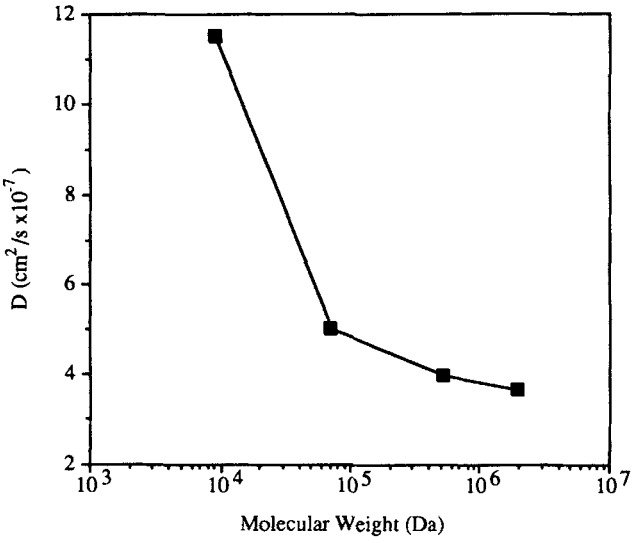

Figure 8. Diffusion coefficients for dextran macromolecules in the absence of protein.

as the double layer surrounding the protein increases, the rate of diffusion also increases. A similar effect was observed by Anderson et al. (1978), who found that rates of gradient diffusion of BSA increase rapidly with decreasing pH at low ionic strength, where the screening of double layer interactions is minimized. The data clearly show that electrostatic charge effects in this system are negligible at KCl concentrations greater than 0.01 M. All data reported below were obtained at a KCl concentration of 0.15 M, thereby eliminating any effects of solute-solute electrostatic interactions. The diffusion coefficient D_0 for BSA in a 0.15 M KCl solution is found to be 7.05×10^{-7} cm^2/s, corresponding to a Stokes-Einstein radius of 3.4 nm, a value that compares very well with the literature value of 3.45 nm (Wattenbarger et al., 1992).

In Figure 7 we show data for the diffusion of BSA in dextran solutions with concentrations that vary from 0 to 7% by weight. Data for dextrans with mean molecular weights of 9.3 kDa, 73, 526 and 2,000 kDa are shown, and are compared with a correlation representing the results of Ogston et al. (1973) for dextrans with a molecular weight of 2,000 kDa. Clearly our results are in good agreement with those of Ogston and coworkers. The data shown are average values from 2-4 experiments, and we estimate the error to be approximately ±7%. To insure that our results for D/D_0 are independent of the

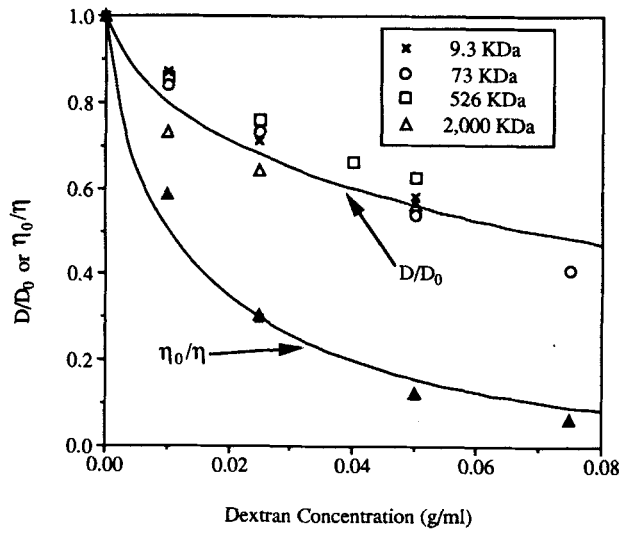

Figure 7. Diffusion coefficient of BSA in solutions of dextran with molecular weights varying from 9.3-2,000 kDa at concentrations ranging from 0 to 7.5% by weight.

The viscosity of the solution of dextran having a molecular weight of 526 kDa is also shown and compared with the prediction of the correlation of Phillies et al. (1989).

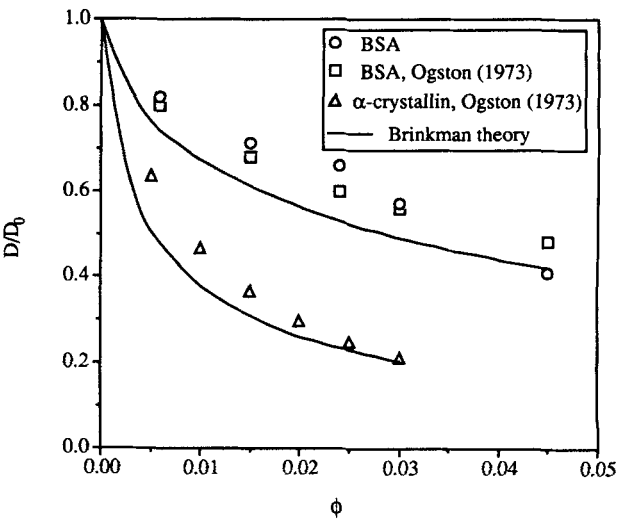

Figure 9. Diffusion coefficients of BSA (averaged over all molecular weights) vs. Brinkman prediction Eq. 4.

Data for the diffusion of BSA and α-crystallin in dextran solutions reported by Ogston et al. (1973) are also shown and compared with the Brinkman prediction.

BSA concentration, we performed additional experiments with 0.5% and 2.5% BSA concentrations by weight in 2% and 5% solutions of 526 kDa dextran, and found no significant difference from the results shown in Figure 7. It would appear that the molecular weight of the dextran molecules has a negligible effect on the rate of diffusion over the range of molecular weights considered here, at least to within the precision of our measurements. We note that Ogston et al. (1973) measured rates of diffusion of α-crystallin (cf. Figure 9) in dextran solutions and similarly found a negligible effect of molecular weight at 500 and 2,000 kDa, but did observe a change at molecular weights as low as 80 kDa.

It is interesting to compare the results for the diffusion of BSA with previously reported results from light scattering studies on the diffusion of latex spheres in dextran solutions (Turner and Hallet, 1976; Phillies et al., 1989). As stated above, the light scattering studies agree rather closely with Eq. 6, which suggests that the dominant effect of the polymer is to increase the viscosity of the solution. Therefore, in addition to the diffusion data just described, we also present data for the viscosity of our solutions of dextran with a molecular weight of 526 kDa. The viscosities were measured by using Canon-Fenske viscometers (Cole-Parmer, Niles, IL). These data are compared with a correlation of viscosity data reported by Phillies et al. (1989), and it is evident that the agreement is excellent. Thus, the viscosities of our solutions are predicted accurately by the correlation of Phillies and coworkers, but our diffusion coefficients D/D_0 are significantly different. Also, our results are independent of the polymer molecular weight, whereas the results for latex sphere diffusion show a significant molecular weight dependence, as does the viscosity. Explanations for these interesting differences are discussed in the next section.

As described earlier, holographic interferometry can be used to measure rates of diffusion for any substance that affects the refractive index. It can therefore be used to measure diffusion coefficients for the dextran molecules themselves, in the absence of any protein solutes. We have measured rates of gradient diffusion for our dextran macromolecules. In these experiments, the lower solution ($x<0$) had a concentration of 5% and the upper solution ($x>0$) had a concentration of 3% polymer by weight (cf. Figure 5). The diffusion coefficients obtained are shown in Figure 8. Interestingly, the polymer macromolecules diffuse as fast as and in some cases faster than the protein. Also, the rate of diffusion depends strongly on molecular weight, as is to be expected for polymer diffusion. These results have implications for hydrodynamic screening models, as discussed below.

Discussion

One approach to providing a theoretical description of diffusion in colloidal systems is to follow the general outline provided by Einstein (1956) for very dilute suspensions, which has since been extended to finite solute volume fractions by Batchelor (1976; 1983). Here solute motion is driven by a "thermodynamic force" equal to the gradient of the chemical potential. In the absence of electrostatic effects, the resistance to the thermodynamic force is just the hydrodynamic drag exerted by the fluid on the moving solute. In such a theory the presence of polymer fibers in the fluid affects diffusion primarily by increasing the hydrodynamic drag on the diffusing solute. Under one possible scenario, the polymer solution can be considered a continuous fluid with a viscosity higher than that of the polymer-free liquid. This description leads one to the prediction of Eq. 6 by a straightforward application of the Stokes-Einstein equation.

Alternatively, the polymer solution can be considered a heterogeneous medium consisting of a liquid permeated by polymer fibers. The diffusing solute moves through the interstices between the fibers, which form a dilute fibrous porous medium. If the fibers are entangled to the point where they do not move in response to the diffusing solute, then they can be modeled by a Kirkwood Riseman or Brinkman model, the two being identical as shown above. One would expect that in the heterogeneous medium the ratio D/D_0 should show a strong dependence on solute size, since solute motion depends on the interfiber spacing being larger than the solute diameter. This dependence is in contrast to the Stokes-Einstein prediction of Eq. 6, in which the solute diameter does not appear.

Of course, these two descriptions lead to the important question of how one knows which mechanism is accurate given the fundamental properties of a particular system. Some insight into this issue can be achieved by considering the distribution of spaces in a random network of straight fibers. This issue has been addressed by Ogston (1958), whose results were later verified and extended by Fanti and Glandt (1990). Ogston's approach involves expanding a spherical surface about each point in a fibrous network. Expansion of each surface ceases when it comes into contact with a fiber, and in this way the radius of a "spherical space" can be assigned to each point in the network. Analysis of the distribution of radii of these spaces in the limit of very long fibers leads to the result (Ogston, 1958)

$$P_{R>a}=\exp\left[-\phi\left(1+\frac{a}{r_f}\right)^2\right], \tag{31}$$

where $P_{R>a}$ is the fraction of the total volume that can accommodate a solute of radius a and r_f is the fiber radius. The very strong dependence of $P_{R>a}$ on solute size in Eq. 31 has implications for how one should conceptualize the diffusion of various solutes in polymer solutions.

First we examine the system used in the experiments discussed in the experimental results section. The Stokes-Einstein radius of bovine serum albumin is 3.45 nm, and we accept previous estimates of the radius of dextran to be approximately 1 nm (Laurent and Killander, 1964; Ogston et al., 1973). By using Eq. 31, we then predict that some 82% of the spaces in the polymer network are accessible to the solute in a 1% polymer solution. It is therefore appropriate to think of a solute diffusing between fibers that form a heterogeneous network. In contrast, if we now consider the light scattering studies done on the diffusion of latex spheres in dextran solutions (Turner and Hallett, 1976; Phillies et al., 1989), we find that the *smallest* spheres used have a radius of 19 nm. This larger radius decreases the fraction of available spaces to less than 2% in a 1% polymer solution; if the polymer volume fraction is increased to just 5%, then $P_{R>a}$ falls to 2×10^{-9}. Clearly the model of a solute moving between fibers is inaccurate in this instance. To the contrary, on the length scale of the latex sphere the polymer network is a homogeneous medium. The sphere cannot move without rupturing entanglements between poly-

mer fibers, just as would happen in, say, a falling ball rheometry experiment. This analysis explains why many groups (cf. introduction) have found that diffusion coefficients measured in this regime agree with Eq. 6, the prediction derived from the Stokes-Einstein equation.

Having examined the geometric differences between the diffusion of proteins and the diffusion of latex spheres in polymer solutions, we return to the former process to examine our experimental results in light of hydrodynamic screening theories. We again assume the polymer network acts as an array of straight fibers with radius $r_f = 1.0$ nm. The hydraulic permeability k (cf. Eq. 4) can be estimated by (Johnson et al., 1987)

$$\frac{k}{r_f^2} = 0.31\phi^{-1.17}, \tag{32}$$

a semi-empirical result that agrees well with other known results for fibrous systems and has been tested extensively for solutions of hyaluronic acid. Using Eq. 32 in conjunction with Eq. 4, one can predict values of D/D_0 for any solute with a known Stokes-Einstein radius. The predictions for BSA diffusing in dextran solutions are compared with our experimental data and with a correlation reported by Ogston et al. (1973) in Figure 9, and the agreement between theory and experiment is excellent given the absence of any adjustable parameters. Here all the data from our experiments are averaged at each polymer concentration, since the BSA diffusion coefficients showed no dependence on dextran molecular weight. Diffusion data for the protein α-crystallin in dextran, reported by Ogston et al. (1973), are also presented, and show the same good agreement with the Brinkman prediction. Note that α-crystallin has a Stokes-Einstein radius of 9.7 nm, almost three times that of BSA. Similar comparisons between the predictions of Eq. 4 and the data for protein diffusion in hyaluronic acid solutions are given by Phillips et al. (1989). All that is needed to make these predictions are the Stokes-Einstein radius of the protein, the volume fraction of polymer and an estimate of the polymer fiber radius.

The success of hydrodynamic screening models in predicting rates of protein diffusion in polymer solutions makes it tempting to conceptualize the process as one where a protein moves randomly through the interstices between entangled and relatively immobile fibers. Indeed, Cukier (1984) states a condition that the fibers be fixed on the time scale of sphere diffusion. However, our measurements of rates of dextran diffusion indicate that the polymer network is dynamic, continually changing its configuration on a time scale comparable to the diffusion time of the protein. Interestingly, the rate of protein diffusion seems to be independent of the rate of dextran diffusion, as evidenced by the fact that D/D_0 for BSA is not significantly affected by the molecular weight of the dextran macromolecules. We note here that we have measured a gradient diffusion coefficient, and that the coefficient governing diffusion in the presence of the BSA, where there is no gradient in dextran concentration, might be lower than the values shown above (cf. Figure 8).

These observations are consistent with the Brinkman model if the fibers, while undergoing a reptation-like movement, are still capable of causing hydrodynamic or Brinkman screening of the type expected in a fibrous porous medium. One explanation for this phenomenon is that the partial constraints on the motion of the reptating macromolecules are sufficient to cause its segments to act as point forces (or point scatterers) rather than as force dipoles or higher-order multipoles when responding to perturbations in the velocity field caused by the diffusing solute. This explanation may indeed be part of the overall picture. However, it has also been shown that Brinkman screening occurs in suspensions of force and torque-free rigid rods (Shaqfeh and Fredrickson, 1990). Shaqfeh and Fredrickson calculate rigorously the propagation tensor for a point force in such a suspension, and they find that on length scales much smaller than the fiber length (but much larger than the fiber radius), the average medium behaves like an effective Brinkman medium and thus screens disturbances with some associated screening length. Further, they report that the average propagator is the same as that for a fibrous porous medium, and that the screening length scales exactly as the Brinkman screening length $k^{1/2}$, where k is the hydraulic permeability for a dilute fibrous medium (cf. Jackson and James, 1986). Thus, the mobile dextran molecules may act as a "configuration-averaged" fibrous porous medium. This hypothesis provides an explanation for why the Brinkman model seems capable of giving accurate predictions with only minimal information about a given system, and without adjustable parameters.

Acknowledgments

The authors gratefully acknowledge the help of Professor André Knoesen in designing the apparatus for holographic interferometry. This work was supported by grant 25690-G7E from the Petroleum Research Fund and by grant BCS-92-09322 from the National Science Foundation.

Notation

C = solute concentration
C_1 = solute concentration in upper, solute-depleted liquid in the diffusion cell
C_2 = solute concentration in lower, solute-rich liquid in the diffusion cell
d = distance between extrema in interferograms
D_0 = diffusion coefficient in pure liquid at infinite dilution
$\hat{F}_i$ = force on the ith singularity
$\hat{K}$ = dimensionless drag coefficient
L = path length of diffusion cell
$\hat{n}$ = dimensionless number density of singularities
N = number of singularities
P = probability density
$\hat{P}$ = dimensionless probability density
$\hat{r}$ = dimensionless position
$\hat{r}_i$ = dimensionless position of ith singularity
R = distance from tube center to gel surface
R_0 = radius of tube
t_0 = time at formation of interface between solute-rich and solute-depleted liquids
t_1 = time when holographic plate is exposed
$t_2 \ldots t_N$ = times when holographic plate is photographed
$\hat{v}$ = dimensionless fluid velocity
$\hat{v}_s$ = velocity field for Stokes flow around a sphere
$\hat{v}'$ = velocity disturbance caused by singularities
$\hat{v}'_i$ = velocity disturbance caused by ith singularity

Greek letters

α = dimensionless parameter for prediction of diffusion coefficients
η = viscosity of a polymer solution
η_0 = viscosity of a pure liquid

ν = dimensionless parameter for prediction of diffusion coefficients

ϕ = fiber or sphere volume fraction

Literature Cited

Altenberger, A. R., M. Tirrell, and J. S. Dahler, "Hydrodynamic Screening and Particle Dynamics in Porous Media, Semidilute Polymer Solutions and Polymer Gels," *J. Chem. Phys.*, **84**, 5122 (1986).

Anderson, J. L., F. Rauh, and A. Morales, "Particle Diffusion as a Function of Concentration and Ionic Strength," *J. Phys. Chem.*, **82**, 608 (1978).

Batchelor, G. K., "Sedimentation in a Dilute Dispersion of Spheres," *J. Fluid Mech.*, **52**, 245 (1972).

Batchelor, G. K., "Brownian Diffusion of Particles with Hydrodynamic Interaction," *J. Fluid Mech.*, **74**, 1 (1976).

Batchelor, G. K., "Diffusion in a Dilute Polydisperse System of Interacting Spheres," *J. Fluid Mech.*, **131**, 155 (1983).

Bochner, N., and J. Pipman, "A Simple Method of Determining Diffusion Coefficients by Holographic Interferometry," *J. Phys. D: Appl. Phys.*, **9**, 1825 (1976).

Berne, B. J., and R. Pecora, *Dynamic Light Scattering*, Krieger, Malabar, FL (1990).

Brown, W., and T. Rymden, "Diffusion of Polystyrene Latex Spheres in Polymer Solutions Studied by Dynamic Light Scattering," *Macromolec.*, **19**, 2942 (1986).

Brown, W., and R. Rymden, "Interaction of (Carboxymethyl)cellulose with Latex Spheres by Dynamic Light Scattering," *Macromolec.*, **20**, 2867 (1987).

Cukier, R. I., "Diffusion of Brownian Spheres in Semidilute Polymer Solutions," *Macromolec.*, **17**, 252 (1984).

Einstein, A., *Investigations on the Theory of the Brownian Movement*, Dover, New York (1956).

Ethier, C. R., "The Hydrodynamic Resistance of Hyaluronic Acid: Estimates from Sedimentation Studies," *Biorheol.*, **23**, 99 (1986).

Ethier, C. R., and R. D. Kamm, "Flow through Partially Gel-Filled Channels," *PhysicoChem. Hydrody.*, **11**, 219 (1989).

Fanti, L. A., and E. D. Glandt, "Partitioning of Spherical Particles into Fibrous Matrices: 1. Density Functional Theory," *J. Colloid Interf. Sci.*, **135**, 385 (1990).

Freed, K. F., and M. Muthukumar, "On the Stokes Problem for a Suspension of Spheres at Finite Concentrations," *J. Chem. Phys.*, **68**, 2088 (1978).

Gabelmann-Gray, L., and H. Fenichel, "Holographic Interferometic Study of Liquid Diffusion," *Appl. Optics*, **18**, 343 (1979).

Jackson, G. W., and D. F. James, "The Permeability of Fibrous Porous Media," *Can. J. Chem. Eng.*, **64**, 364 (1986).

Jain, R. K., R. J. Stock, S. R. Chary, and M. Rueter, "Convection and Diffusion Measurements Using Fluorescence Recovery after Photobleaching and Video Image Analysis—Invitro Calibration and Assessment," *Microvascular Res.*, **39**, 77 (1990).

Johnson, M., R. Kamm, C. R. Ethier, and T. Pedley, "Scaling Laws and the Effects of Concentration Polarization on the Permeability of Hyaluronic Acid," *PhysicoChem. Hydrody.*, **9**, 427 (1987).

Kim, S., and S. J. Karrila, *Microhydrodynamics*, Butterworth-Heinemann, Stoneham, MA (1991).

Kim, S., and W. B. Russel, "Modelling of Porous Media by Renormalization of the Stokes Equations," *J. Fluid Mech.*, **154**, 269 (1985).

Kosar, T. F., "Measurement of Hindered Diffusion by Holographic Interferometry," MS Thesis, Univ. of California, Davis (1993).

Langevin, D., and F. Rondelez, "Sedimentation of Large Colloidal Particles through Semidilute Polymer Solutions," *Polymer*, **19**, 875 (1978).

Laurent, T. C., I. Bjork, A. Pietruszkiewicz, and H. Persson, "On the Interaction between Polysaccharides and Other Macromolecules: II. The Transport of Globular Particles through Hyaluronic Acid Solutions," *Biochimica et Biophysica Acta*, **49**, 258 (1961).

Laurent, T. C., and Hakan Persson, "On the Interaction between Polysaccharides and Other Macromolecules: III. The Use of Hyaluronic Acid for the Separtion of Macromolecules in the Ultracentrifuge," *Biochimica et Biophysica Acta*, **78**, 360 (1963).

Laurent, T. C., and J. Killander, "A Theory of Gel Filtration and Its Experimental Verification," *J. Chromatog.*, **14**, 317 (1964).

Liron, N., and R. Shahar, "Stokes Flow Due to a Stokeslet in a Pipe," *J. Fluid Mech.*, **86**, 727 (1978).

Mustafa, M., and P. S. Russo, "Nature and Effects of Nonexponential Correlation Functions in Probe Diffusion Experiments by Quasi-elastic Light Scattering," *J. Colloid Interf. Sci.*, **129**, 240 (1989).

Ogston, A. G., "The Spaces in a Uniform Random Suspension of Fibres," *Trans. Farad. Soc.*, **54**, 1754 (1958).

Ogston, A. G., G. N. Preston, and J. D. Wells, "On the Transport of Compact Particles through Solutions of Chain-Polymers," *Proc. R. Soc. Lond. A*, **333**, 297 (1973).

Onyenemezu, C. N., M. Roman, D. Gold, and W. G. Miller, "Diffusion of Polystyrene Latex Particles in Polystyrene Matrix Solutions: Effect of Matrix Molecular Weight and Solvent Quality," ACS Meeting, Chicago (1993).

Phillies, G. D. J., "The Hydrodynamic Scaling Model for Polymer Self-Diffusion," *J. Phys. Chem.*, **93**, 5029 (1989).

Phillies, G. D. J., and D. Clomenil, "Probe Diffusion in Polymer Solutions under Theta and Good Conditions," *Macromolec.*, **26**, 167 (1993).

Phillies, G. D. J., J. Gong, L. Li, A. Rau, K. Zhang, L. Yu, and J. Rollings, "Macroparticle Diffusion in Dextran Solutions," *J. Phys. Chem.*, **93**, 6219 (1989).

Phillips, R. J., W. M. Deen, and J. F. Brady, "Hindered Transport of Spherical Macromolecules in Fibrous Membranes and Gels," *AIChE J.*, **35**, 1761 (1989).

Phillips. R. J., W. M. Deen, and J. F. Brady, "Hindered Transport in Fibrous Membranes and Gels: Effect of Solute Size and Fiber Configuration," *J. Colloid Interf. Sci.*, **139**, 363 (1990).

Pu, Z., and W. Brown, "Translational Diffusion of Large Silica Spheres in Semidilute Polyisobutylene Solutions," *Macromolec.*, **22**, 890 (1989).

Rubinstein, J., "Effective Equations for Flow in Random Porous Media with a Large Number of Scales," *J. Fluid Mech.*, **170**, 379 (1986).

Ruiz-Bevia, F., J. Fernandez-Sempere, and J. Colom-Valiente, "Diffusivity Measurement in Calcium Alginate Gel by Holographic Interferometry," *AIChE J.*, **35**, 1895 (1989).

Seufert, W. D., and R. N. O'Brien, "Determination of Diffusion Coefficients from the Progression of Interference Fringes," *J. Phys. Chem.*, **88**, 829 (1984).

Shaqfeh, E. S. G., and G. H. Fredrickson, "The Hydrodynamic Stress in a Suspension of Rods," *Phys. Fluids A*, **2**, 7 (1989).

Stewart, U. A., M. S. Bradley, and C. S. Johnson Jr., "Transport of Probe Molecules through Fibrin Gels as Observed by Means of Holographic Relaxation Methods," *Biopolym.*, **27**, 173 (1988).

Szydlowska, J., and B. Janowska, "Holographic Measurement of Diffusion Coefficients," *J. Phys. D: Appl. Phys.*, **15**, 1385 (1982).

Tracy, M. A., J. L. Garcia, and R. Pecora, "An Investigation of the Microstructure of a Rod/Sphere Composite Liquid," *Macromolec.*, **26**, 1862 (1993).

Tracy, M. A., and R. Pecora, "Dynamics of Rigid and Semirigid Rodlike Polymers," *Ann. Rev. Phys. Chem.*, **43**, 525 (1992).

Tracy, M. A., and R. Pecora, "Application of Probe Diffusion Models to Sphere Diffusion in a Rod/Sphere Composite Liquid," *Proc. SPIE*, **1884**, 88 (1993).

Turner, D. N., and F. R. Hallett, "A Study of the Diffusion of Compact Particles in Polymer Solutions using Quasi-Elastic Light Scattering," *Biochimica et Biophysica Acta*, **451**, 305 (1976).

Tyrrell, H. J. V., and K. R. Harris, *Diffusion in Liquids*, Butterworths, Boston (1984).

Wattenbarger, M. R., V. A. Bloomfield, Z. Bu, and P. S. Russo, "Tracer Diffusion of Proteins in DNA Solutions," *Macromolec.*, **25**, 5263 (1992).

Weast, R. C., and M. J. Astle, *CRC Handbook of Chemistry and Physics*, CRC Press, Boca Raton, FL (1980).

Wiegel, F. W., *Fluid Flow Through Porous Macromolecular Systems*, **121**, Springer Verlag, New York (1980).

Manuscript received Dec. 22, 1993, and revision received Mar. 28, 1994.